Dalton Transactions

PAPER

View Article Online
View Journal

Cite this: DOI: 10.1039/c8dt04960b

Revisiting the reactivity of tetrachloroauric acid with *N,N*-bidentate ligands: structural and spectroscopic insights†

R. Tyler Mertens, Jong Hyun Kim, Will C. Jennings, Sean Parkin and Samuel G. Awuah *

Received 17th December 2018,
Accepted 7th January 2019

DOI: 10.1039/c8dt04960b

rsc.li/dalton

The reactivity of tetrachloroauric acid ($HAuCl_4$) with readily accessible bidentate N-donor ligands affords *N,N*-ligated Au(III) center complexes. These compounds are useful precursors of stable catalysts, anticancer agents, and building blocks for materials. This report provides detailed insight into intermediates, equilibria, the counter anion effect, and structural variability, using spectroscopy, crystallography and computational tools. Novel mixed-valence Au(I) and Au(III) complexes $[Au(o\text{-phen})Cl_2]_2[AuCl_2][AuCl_4]$ and $[Au(o\text{-phen})Cl_2][AuCl_2]$ having $AuCl_2^-$ and $AuCl_4^-$ anions linearly arranged in the axial sites of the square-planar $Au(o\text{-phen})Cl_2$ cation were discovered. Other competing side products of the reaction studied revealed protonated *N,N*-bidentate ligands with $AuCl_4^-$ anions. Quantitative variable temperature NMR studies reveal that for a mixture of target Au(III) salt and the protonated ligand, the reaction favors the irreversible formation of the side product. Using a rapid (30 min) temperature controlled protocol, the desired coordinated species is accessible in respectable yields while avoiding side products.

Introduction

Gold complexes possess enormous utility due to their unique relativistic and electrochemical behavior.[1–4] These complexes act as carbophilic Lewis acids that readily interact with nucleophilic and π-activated systems, such as alkenes and alkynes.[5–7] This has led to an ignition of gold chemistry in catalysis and biology, with the dominant use of Au(I) and Au(III) complexes. Gold(III) reagents are isoelectronic to platinum(II) in the $5d^8$ configuration and can be subjected to ligand variability with mono- and poly-dentate ligands in ways superior to gold(I). Owing to this distinguishing feature, bidentate coordinating ligands to stabilize and tune the reactivity of the Au(III) center (Chart 1) have become very attractive. The oxalates, phosphines, dithiolates, and heterocyclic *N,N*-bidentates, including 1,10-*o*-phenanthroline, 2,2′-bipyridine, and bathophenanthroline, are such ligand systems.[8–14] Recent intensified efforts in redox gold catalysis and gold-containing antiarthritic and anticancer drugs make investigating the chemistry of gold in solution imperative.[11,15,16]

In gold catalysis, bidentate N-donor ligands have been used as additives. These commonplace ligands play crucial roles in the rudimentary stages of the organogold chemistry including oxidative addition, trans-metalation, and reductive elimination.[17,18] Additionally, square-planar bipyridyl ligated gold(III) complexes exhibit potent anticancer activity in cells and weak DNA binding properties.[15] The use of dinuclear gold(III) oxo complexes bearing phenanthroline bipyridyl ligands shows interesting antiproliferative effects with protein binding to serum albumin, cytochrome c, ubiquitin, and histone deacetylase inhibition.[19,20]

The reactions of gold(III) with bidentate coordinating ligands first reported by Block *et al.* investigated the use of aliphatic diamines such as 1,2-ethanediamine and 1,2-propanediamine as well as heterocyclic N-donor ligands, including 2,2-bipyridine and phenanthroline.[21] Ever since, a significant

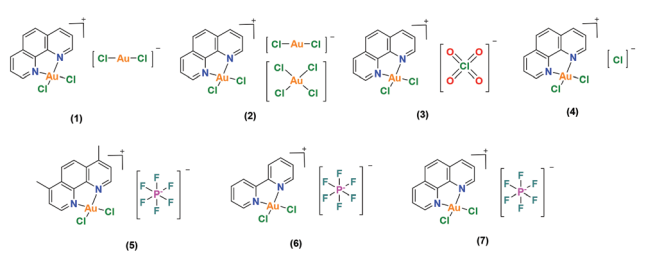

Chart 1 Bipyridyl ligated Au(III) complexes, **1–7**.

Department of Chemistry, University of Kentucky, 505 Rose Street, Lexington, Kentucky 40506, USA. E-mail: awuah@uky.edu

†Electronic supplementary information (ESI) available: Spectroscopic data, crystallographic information, and data from DFT calculations can be found. CCDC 1868472–1868477 for **1–6**. For ESI and crystallographic data in CIF or other electronic format see DOI: 10.1039/c8dt04960b

body of work has employed this reaction method with slight variations using different *N*,*N*-bidentate ligands.[22,23] Initial mechanistic work to elucidate ligand substitution in gold-based square planar complexes has employed Au(III) amine complexes. In addition, whereas the aqueous solution chemistry and structural investigations of Au(III) complexes bearing tridentate amine and terpyridine ligands have been well studied,[15,19,24,25] mechanistic investigation of Au(III) complexes supported by bidentate ligands will expand our understanding of their overall reactivity.[22,23,26–30]

We report the preparation of Au(III) complexes bearing heterocyclic N-donor ligands by a streamlined rapid synthetic protocol and offer detailed insights into structural characterization *via* X-ray crystallography. In this report, we discovered novel mixed valence Au(I)–Au(III) complexes. Furthermore, isolation of protonated ligands demonstrates that the hydrolysis of $HAuCl_4$ lowers the pH of the reaction medium leading to protonated ligands as byproducts. Our temperature-controlled method described in this report circumvents the formation of byproducts.

Experimental methods

General considerations

All reagents were purchased from Oakwood chemicals, VWR, Acros Organics, Alfa Aesar, and TCI and used as received. All reactions were carried out under normal atmospheric conditions in a fume hood. Compounds **1–6** were synthesized by a rapid temperature-controlled protocol. Protonated compounds were formed by following literature procedures.[31–33]

Physical measurements

Deuterated solvents were purchased from Cambridge Isotope Laboratories (Andover, MA). ^{1}H NMR spectra were recorded on a Varian Unity 400 NMR spectrometer with a Spectro Spin superconducting magnet in the University of Kentucky NMR facility. Chemical shifts in ^{1}H NMR spectra were internally referenced to solvent signals (^{1}H NMR: DMSO at δ = 2.50 ppm and CD_3CN at δ = 1.94, ^{13}C NMR: DMSO at δ = 39.52 ppm and CD_3CN at δ = 118.7 ppm, 1.39 ppm), and those in ^{31}P NMR spectra were externally referenced to 85% H_3PO_4 in D_2O (δ = 0 ppm). Electrospray ionization mass spectrometry (ESI-MS) was performed on an Agilent Technologies 1100 series liquid chromatography/MS instrument. High-resolution mass spectra (HRMS) were obtained by direct flow injection (injection volume = 5 or 2 μL) ElectroSpray Ionization (ESI) on a Waters Qtof API US instrument in the positive mode (CIC, Boston University). Typical conditions are as follows: capillary = 3000 kV, cone = 35 volts or 15 volts, source temperature = 120 °C, and desolvation temperature = 350 °C. Elemental analyses for **2**, **4** and **7** were performed by Atlantic microlabs (commercial laboratory).

Synthesis of [Au(phen)Cl_2][$AuCl_2$] (1)

Phenanthroline monohydrate (267 mg, 1.35 mmol) was added to a solution of tetrachloroauric(III) acid trihydrate (197 mg, 0.5 mmol) in 10 mL of ethanol. The solution was placed on a rotary evaporator and heated at 72 °C for 10 minutes. The precipitate that formed changed color from yellow to orange within the course of the reaction. The precipitate was filtered and washed with ether (10 mL × 3). Crystals were grown using DMF/ether. Yield: 307 mg, 80%. ^{1}H NMR (400 MHz, MeCN-d_3) δ 9.66 (d, J = 4.4 Hz, 2H), 9.16 (d, J = 7.2 Hz, 2H), 8.38 (s, 2H), 8.30 (t, J = 7.2 Hz, 2H). ^{13}C NMR (400 MHz, DMSO-d_6) δ 148.60, 148.13, 145.01, 132.96, 129.41, 128.03. MS (*m*/*z*, EI HRMS): [M + H]. Calcd for $C_{12}H_8N_2Cl_4Au_2$ 716.8821, found 716.8822.

Synthesis of [Au(phen)Cl_2]$_2$[$AuCl_4$][$AuCl_2$] (2)

Phenanthroline monohydrate (557 mg, 2.81 mmol) and tetrachloroauric(III) acid trihydrate (539.5 mg, 1.37 mmol) were added together in 35 mL of ethanol. A yellow precipitate formed immediately and the solution was placed on a rotary evaporator and heated at 72 °C for 10 minutes. The color of the precipitate turned from yellow to orange and the reaction was stopped after 30 min. Yield: 58 mg, 11%. ^{1}H NMR (400 MHz, MeCN-d_3) δ 9.66 (d, J = 6.0 Hz, 2H), 9.16 (d, J = 8.4 Hz, 2H), 8.38 (s, 2H), 8.30 (t, J = 7.2 Hz, 2H). ^{13}C NMR (400 MHz, DMSO-d_6) δ 156.12, 147.47, 146.07, 130.05, 127.04, 123.40. Anal calcd for $C_{12}H_8Au_2Cl_5N_2$: C, 19.18; H, 1.07; N, 3.73. Found: C, 19.57; H, 1.33; N, 3.93.

Synthesis of [Au(phen)Cl_2][ClO_4] (3)

Phenanthroline monohydrate (60.4 mg, 0.305 mmol) and tetrachloroauric(III) acid trihydrate (100 mg, 0.254 mmol) were added to 10 mL of ethanol and sonicated for 10 minutes. Sodium perchlorate (93 mg, 0.762 mmol) was added to the mixture and further sonicated for 5 min. The solution was refluxed at 80 °C for 12 h. The precipitate was filtered and washed with ether. Crystals were grown by slow diffusion of DMF/ether. Bulk purification was achieved by dissolving the crude solid in acetonitrile followed by centrifugation of the undissolved salt. The solution was then decanted out and dried under vacuum to give complex **3**. Yield: 92 mg, 62%. ^{1}H NMR (400 MHz, MeCN-d_3) δ 9.67 (d, J = 4.0 Hz, 2H), 9.15 (d, J = 4.0 Hz, 2H), 8.38 (s, 2H), 8.33 (t, J = 1.6 Hz, 2H). ^{13}C NMR (400 MHz, DMSO-d_6) δ 148.60, 148.1, 145.0, 132.96, 129.41, 128.07.

Synthesis of [Au(phen)Cl_2][Cl] (4)

To an ethanolic solution (14 mL) of tetrachloroauric(III) acid trihydrate (199 mg, 0.51 mmol) was added phenanthroline monohydrate (202 mg, 1.02 mmol) and placed on the rotovap. While stirring, the solution was heated to 72 °C for 30 min. The solution was cooled and then filtered to leave behind a light-orange colored solid. The collected solid was washed with ether and ethanol and dried under vacuum. Yield: 76 mg, 31%. ^{1}H NMR (400 MHz, DMSO-d_6) δ 9.70 (d, J = 4.0 Hz, 2H), 9.36 (d, J = 4.0 Hz, 2H), 8.53 (s, 2H), 8.43 (t, J = 16.0 Hz, 2H). ^{13}C NMR (400 MHz, DMSO-d_6) δ 148.08, 142.47, 137.87, 130.07, 128.02, 126.21. Anal calcd for $C_{12}H_8AuCl_3N_2$: C, 29.81; H, 1.67; N, 5.79. Found: C, 30.05; H, 1.66; N, 5.75.

[Au(4,7-Dmp)Cl$_2$][PF$_6$] (5)

4,7-Dimethylphenanthroline, (4,7-dmp), (319.7 mg, 0.141 mmol), tetrachloroauric(III) acid trihydrate (503 mg, 1.28 mmol), and ammonium hexafluorophosphate (417 mg, 2.56 mmol) were dissolved in 25 mL of an ethanol/water mixture 2 : 1 and sonicated for 1 min. The mixture was placed on a rotovap and heated at 72 °C while rotating for 30 minutes. The solution was cooled and filtered to leave behind a dull yellow solid, which was washed with ethanol (10 mL × 3) and then with ether (10 mL × 3). Yield: 725 mg, 81%. ^{1}H NMR (400 MHz, DMSO-d_6) δ 9.55 (d, J = 8.0 Hz, 2H), 8.57 (s, 2H), 8.27 (d, J = 8.0 Hz, 2H), 3.09 (s, 6H). ^{13}C NMR (400 MHz, DMSO-d_6) δ 156.72, 147.67, 145.47, 132.38, 127.94, 126.34, 19.78. ^{31}P NMR (400 MHz, DMSO-d_6) δ −130.66, −135.05, −139.44, −143.84, −148.23, −152.62.

Synthesis of [Au(bpy)Cl$_2$][PF$_6$] (6)

Bipyridine (207.1 mg, 0.1.33 mmol), tetrachloroauric(III) acid trihydrate (469.8 mg, 1.19 mmol), and ammonium hexafluorophosphate (392.5 mg, 2.41 mmol) were dissolved in 16 mL of a 2 : 1 ethanol/water mixture and sonicated for 1 min. The mixture was placed on a rotovap and heated at 72 °C while rotating for 30 minutes. The solution was cooled and filtered to leave behind a bright, fluffy yellow powder, which was washed with ethanol (10 mL × 3) and then with ether (10 mL × 3). Yield: 529 mg, 84%. ^{1}H NMR (400 MHz, DMSO-d_6) δ 9.41 (d, J = 4.0 Hz, 2H), 8.93 (d, J = 8.0 Hz, 2H), 8.40 (t, J = 8.0 Hz, 2H), 8.14 (t, J = 8.0 Hz, 2H). ^{13}C NMR (400 MHz, DMSO-d_6) δ 156.12, 149.84, 147.70, 147.47, 146.07, 141.99, 130.05, 127.04, 126.91, 123.40. ^{31}P NMR (400 MHz, DMSO-d_6) δ −130.66, −135.05, −139.44, −143.84, −148.23, −152.62.

Synthesis of [Au(phen)Cl$_2$][PF$_6$] (7)

Phenanthroline monohydrate (172.3 mg, 0.870 mmol), tetrachloroauric(III) acid trihydrate (302 mg, 0.767 mmol), and ammonium hexafluorophosphate (258.8 mg, 1.59 mmol) were dissolved in 20 mL of a 2 : 1 ethanol/water mixture and sonicated for 1 min. The mixture was placed on a rotovap and heated at 72 °C while rotating for 1.5 hours. The solution was cooled and filtered to leave behind a bright yellow solid, which was washed with ethanol (10 mL × 3) and then with ether (10 mL × 3). Yield: 287 mg, 63%. ^{1}H NMR (400 MHz, MeCN-d_3) δ 9.69 (d, J = 8.0 Hz, 2H), 9.17 (d, J = 8.0 Hz, 2H), 8.40 (s, 2H), 8.34 (t, J = 6.0 Hz, 2H). ^{13}C NMR (400 MHz, DMSO-d_6) δ 148.22, 142.61, 138.01, 130.21, 128.16, 126.36. ^{31}P NMR (400 MHz, MeCN-d_3) δ −135.41, −139.80, −144.19, −152.98, −157.36. Anal calcd for $C_{12}H_8AuCl_2N_2PF_6$: C, 24.30; H, 1.36; N, 4.72. Found: C, 24.57; H, 1.33; N, 4.73.

Synthesis of [Hphen][AuCl$_4$]

Phenanthroline monohydrate (0.620 mmol) and tetrachloroauric(III) acid trihydrate (0.507 mmol) were added to 10 mL of ethanol and sonicated for 10 min. Sodium perchlorate or ammonium hexafluorophosphate (1.524 mmol) was added and the mixture was further sonicated for 5 minutes. The solution was refluxed at 85 °C for 4 hours. The solid collected was dissolved in DMF and ether was slowly diffused into the solution. Two types of crystals were isolated and examined by X-ray diffraction. The two structures found were **3** or **7** and the protonated phenanthroline gold salt.

X-ray crystallography

Crystals of **1–6** (Table S1†) were grown at room temperature by vapor diffusion of diethyl ether into a DMF or MeCN solution of each complex. All crystals were mounted using polyisobutene oil on the tip of a fine glass fibre, which was fastened in a copper mounting pin with an electrical solder. It was placed directly into the cold gas stream of a liquid-nitrogen based cryostat.[34,35] A Bruker D8 Venture diffractometer with graded-multilayer focused MoKα X-rays (λ = 0.71073 Å) was used to collect diffraction. Raw data were integrated, scaled, merged, and corrected for Lorentz-polarization effects using the APEX3 package.[36–38] Space group determination and structure solution and refinement were carried out with SHELXT and SHELXL,[39,40] respectively. All non-hydrogen atoms were refined with anisotropic displacement parameters. Hydrogen atoms were placed at calculated positions and refined using a riding model with their isotropic displacement parameters (U_{iso}) set to either 1.2U_{iso} or 1.5U_{iso} of the atom to which they were attached. Ellipsoid plots were drawn using SHELXTL-XP[41] The structures, deposited in the Cambridge Structural Database, were checked for missed symmetry, twinning, and overall quality with PLATON,[42] an R-tensor,[43] and finally validated using CheckCIF.[42]

Results and discussion

Solution chemistry of HAuCl$_4$

Reaction optimization towards the formation of bipyridyl ligated Au(III) complexes is needed to minimize protonolysis and increase yield. Furthermore, understanding the reactivity of tetrachloroauric acids with N-donor ligands in solution is crucial for effective utilization of these building blocks in gold chemistry.[11,15,44–46] Our quest to elucidate the reactivity of HAuCl$_4$ or NaAuCl$_4$ with *N*,*N*-bipyridyl ligands led to the discovery of new coordinated Au(III) species with gold counter anions (AuCl$_2$ or AuCl$_2$/AuCl$_4$). Mixed valence Au(I) and Au(III) complexes following the reaction of HAuCl$_4$ with representative bipyridyl ligands such as phenanthroline demonstrate the broad spectrum of possible complexes, which require further investigation. Previous reports showed the formation of [Au(phen)Cl$_2$]AuCl$_4$ or [Au(phen)Cl$_2$]Cl complexes. For example, the reaction by Block *et al.* was carried out in ethyl alcohol and heated on a steam cone for 4 h.[21] Other methods have also optimized the methodology by using different solvents, such as acetonitrile or a mixture of water and ethyl alcohol. Here, we describe a short temperature-controlled method that leads to the formation of [Au(phen)Cl$_2$]Cl as well as mixed valence Au(I)/Au(III) complexes of the type, [Au(phen)Cl$_2$][AuCl$_2$], **1** and [Au(phen)Cl$_2$]$_2$[AuCl$_2$][AuCl$_4$], **2** if no additives are used

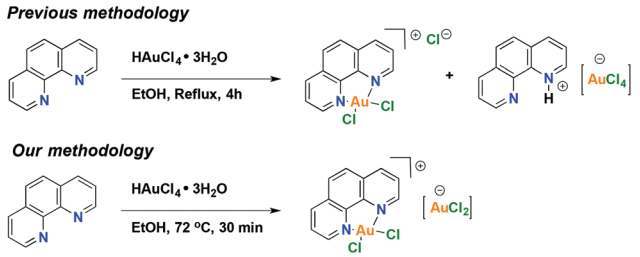

Fig. 1 Representative reaction scheme of the previously reported reaction of *N*,*N*-bipyridyl ligands and our temperature-controlled method.

(Fig. 1). The solvent used may likely be a reductant for the described reaction.

When we reacted $HAuCl_4{\cdot}3H_20$ and 1,10-phenanthroline monohydrate in ethanol under reflux conditions for 4 h, the yellow-orange precipitates were recrystallized to obtain a coordinated Au(III) complex with Au(I) counter anions, **1**. Upon analysis of the filtrate of this reaction using GC-MS (Fig. S19 and S20†), a *m*/*z* value corresponding to free phenanthroline was found. This reveals that all reduction of Au(III) to Au(I) occurs by means of the ligand and no other products are formed. Evidence of any other Au(I) species was not found. Moreover, the isolated yellow precipitate comprised complex **1**, and a protonated phenanthroline ligand with an $[AuCl_4]^-$ counter ion. With the use of NMR, we confirmed the instantaneous formation of bright yellow precipitates following the addition of an ethanolic solution of $HAuCl_4$ and phenanthroline at room temperature was the protonated ligand. This was subsequently confirmed by single-crystal X-ray diffraction. The irreversibility of the reaction was therefore established by the characterization of products and analysis of the filtrate. To address the issue of unwanted side products, we resorted to controlling the temperature and duration of the reaction. Thus, we reasoned that the strong coordinating effect of N-donor ligands from bidentate species may not warrant high temperatures and longer reaction times as commonly reported.[21] Thus, to an ethanolic solution of $HAuCl_4$ were added respective bipyridyl ligands and the yellow solution was warmed to 72 °C and stirred for 30 min. The reaction generated single crystals of both **1** and **2** (Table S1†). An equimolar stoichiometric ratio of $HAuCl_4$ and phenanthroline at 70 °C for 10 min makes the formation of $[Au(phen)Cl_2]Cl$, **4**, possible[47] as confirmed by X-ray crystallography.

To investigate the effect of alkali salts on the reaction methodology described (*supra*), we utilized $NaAuCl_4{\cdot}2H_2O$ and phenanthroline as reactants. The reaction of equimolar amounts of $NaAuCl_4{\cdot}2H_2O$ and phenanthroline proceeded in ethanol under reflux conditions for 4 h. A mixture of coordinated Au(III) and protonolysis of the phenanthroline ligand were observed (Fig. S21 and S22†). In contrast, the reaction with phenanthroline and $NaAuCl_4{\cdot}2H_2O$ following our methodology yielded complex **1** exclusively (Fig. S21 and S22†). Regardless of the Au(III) starting material, protonation of phenanthroline occurred, which can be attributed to the abundance of protons in the solvent or starting materials. To eliminate protonation from the solvent and the atmosphere, the same reaction was carried out under inert conditions using dry acetonitrile. The precipitate obtained again revealed protonation of the phenanthroline ligand, despite the use of dry conditions. The Au(III) starting material exists as hydrate salts and is the potential source of protonation.

Control of counter ions in these gold compounds is essential to avoid the presence of precious Au-containing counter anions. Potentiation of counter ions can be achieved by the use of additives to improve ionic strength. We therefore considered the use of perchlorate or hexafluorophosphate salts as additives and their impact on the formation of ligated bipyridyl Au(III). In this approach, we reacted $HAuCl_4$ with phenanthroline in the presence of ethanol and excess $[ClO_4]^-$ or $[PF_6]^-$ salts. The identity of anions in these compounds was confirmed by X-ray crystallography and NMR in the case of $[PF_6]^-$ salt.[48] When the reaction was subjected to high temperature, 100 °C for 4 h, the protonated N-donor ligand in addition to the expected $[Au(phen)Cl_2][X]$, where X is $[ClO_4]^-$ or $[PF_6]^-$, was formed.

Recrystallization from acetonitrile gave pure $[Au(phen)Cl_2][X]$. This purification approach is not applicable to complexes with gold counter ions; hence there is a need for optimization of reaction conditions to access distinct complexes. To avoid the purification steps, and improve yields, we subjected the reaction to our temperature-controlled protocol (72 °C for 30 min), giving rise to the desired complexes in ~80% yield. For example, we used $[PF_6]$ as the additive in the synthesis of complexes **5** and **6**, which bear 4,7-dimethylphenanthroline and 2,2′-bipyridine ligands, respectively. The yields of these reactions were >80%. Overall, using additives such as $[ClO_4]^-$, $[PF_6]^-$, or $[BF_4]^-$ eliminates the presence of gold-containing sacrificial counter ions.

The pH of a solution of $HAuCl_4$ is acidic, which leads to the instantaneous formation of the protonated salts. Adjusting the pH to a more basic solution with a 1 M $NaOH_{(ethanol)}$ solution to a pH above 7 resulted in reduction to elemental gold. There is no optimal pH that controls the amount of protonated salt formed during the reaction; however, maintaining the pH at 2–5 reduced the formation of the protonated salts but not completely. Mixed valence Au(III) compounds arise predominantly from reactions that utilize a slight excess (2.5 equivalents) of $HAuCl_4$. Keeping this stoichiometric ratio under acidic conditions (pH = 2) results in the formation of $[Au(phen)Cl_2][AuCl_4]$. Generally, an equimolar reaction of $HAuCl_4$ and phenanthroline leads to **4** as a bright yellow solid instead of the yellowish-orange color for mixed valence complexes or Au(III) compounds with $[AuCl_2]^-$ or $[AuCl_4]^-$ counter ions. Solution chemistry studies using Au(III) dien[49] compounds as well as Au(III) terpyridine[24] showed that pH affects product formation. Our present studies provide a comprehensive insight into the factors that affect the reactivity of $HAuCl_4$ with bipyridyl ligands in solution, different products formed, and ways to access predominantly *N*,*N*-bipyridyl Au-ligated complexes. The methods most widely used to obtain $[Au(phen)Cl_2]Cl$ and its

derivatives in the literature produce protonated bipyridyl ligands with respective sacrificial gold counter-anions. Furthermore, we investigated the dependence of pH on product formation and importantly, the elimination of protonated ligands.

There have been few reports of such protonated ligands in the literature,[46,50–52] but our studies reveal that temperature shifts the equilibrium more to the protonated ligands. We confirmed this by variable temperature NMR studies using a mixture of $[Au(phen)Cl_2]ClO_4$ and $[Au(phen)H]ClO_4$ or $[Au(phen)Cl_2]PF_6$ and $[Au(phen)H]PF_6$ in DMSO-d_6 from 22 °C to 75 °C and X-ray crystallography to unambiguously differentiate target compounds from side products.

Temperature dependence and variable temperature studies

Following the reaction of an equimolar ratio of $HAuCl_4$ and phenanthroline in ethanol for 4 h at 100 °C in the presence of excess additive $[ClO_4]^-$ or $[PF_6]^-$, 10% protonated ligand was observed by NMR (Fig. 2 and S23†). Using variable temperature NMR, we sought to understand the stability of generated species within the reaction. Variable temperature proton NMR studies were performed on a Varian Unity 400 NMR spectrometer with a Spectro Spin superconducting magnet. Complexes **3** and **7** were chosen for VT-NMR studies. The mixture was subjected to variable temperature NMR in DMSO-d_6 from 22 °C–75 °C. It was observed that at 75 °C there was nearly complete conversion to the protonated species. This can be attributed to the cleavage of the Au–N bonds at high temperature and subsequent protonation of the ligand by water in the NMR solvent or reaction medium.

The study reveals conversion of the Au(III) complex to its corresponding protonated phenanthroline salt. The conversion of the gold complex to its corresponding salt was not affected by the particular counterion present. Taken together, this explains the presence of protonated ligands when reactions are subjected to high temperatures (100 °C) for 4 h.

Quantitative variable temperature NMR

Quantitative VT ^{1}H NMR was performed using complex **3** to study the change in the amount of the Au(III) complex and corresponding protonated phenanthroline salt using trimethoxybenzene as the internal standard. For quantification, the most deshielded proton of **3** (9.71 ppm) or [H-phen][ClO_4] (9.32 ppm) was used in reference to the aromatic peak (6.09 ppm) of trimethoxybenzene (Fig. S24–S28†). The area under each denoted proton was integrated at the same values for the duration of the experiment. Initially, 0.038 mmol of **3** and 0.051 mmol of the standard were placed in an NMR tube and subjected to variable temperature studies. After the sample had been heated to 80 °C and cooled back to room temperature, 0.00 mmol of **3** was found and 0.038 mmol of the corresponding phenanthroline salt was left in the NMR sample (Fig. 3). This reveals that the Au(III) complex is stoichiometrically converted to the corresponding phenanthroline salt.

A plot of mmol *versus* temperature reveals rapid conversion of complex (**3**) to the corresponding protonated salt. Once the NMR solution had been re-cooled to 20 °C, the solution was subjected to direct temperature ramp back to 80 °C to study the reversibility of the process. The study showed that 0.038 mmol of [H-phen][ClO_4] was still observed, indicating that even with good mass balance, the process is irreversible. This explains why a substantial amount of protonated salts can be found in the crude product for reactions performed under high temperature conditions for 4 h and upon formation, persist in the reaction mixture due to the irreversible nature of the protonolysis event.

X-ray structures of 1 and 2

The coordinated phenanthroline Au(III) complex bearing the $[AuCl_2]^{-1}$ counterion, **1**, was solved from a yellow slab, dimensions of 0.060 × 0.050 × 0.030 mm, which was grown by slow diffusion of diethyl ether into DMF (Fig. 4). The structure was

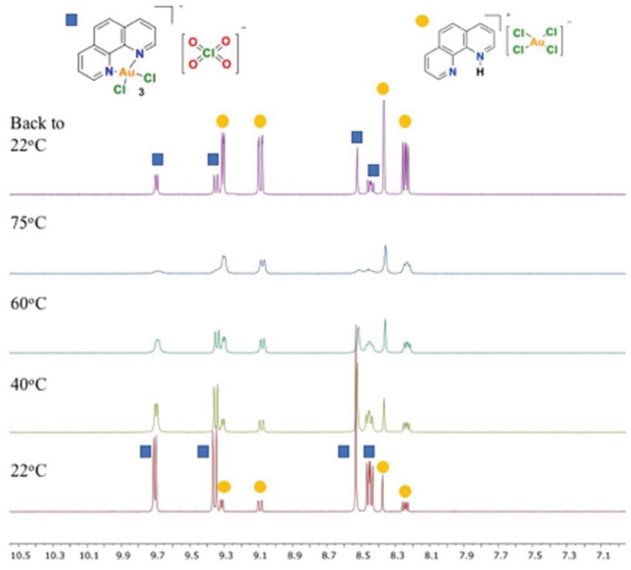

Fig. 2 VT H^1 NMR study of the complex, **3**, at temperatures 22 °C, 40 °C, 60 °C, and 75 °C, followed by a scan once cooled back to 22 °C.

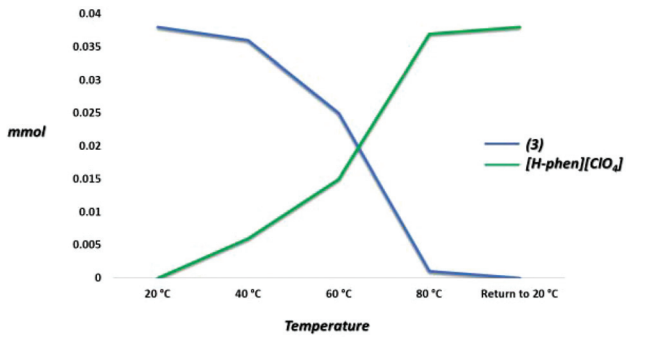

Fig. 3 Q-VT-^{1}H NMR of compound **3**. Temperature ramp was as indicated. Total conversion is observed with a decrease in **3** (blue) and formation of [H-phen][ClO_4] (green). The plot is an average of two independent experiments with insignificant error.

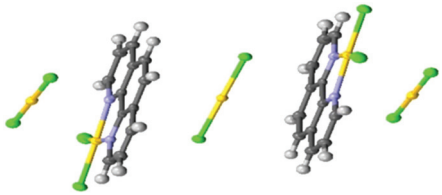

Fig. 4 An ellipsoid plot showing a stack along the *c*-axis of alternating cations and anions. All non-hydrogen atoms are drawn with an ellipsoid of 50% probability. Hydrogen atoms were omitted for clarity.

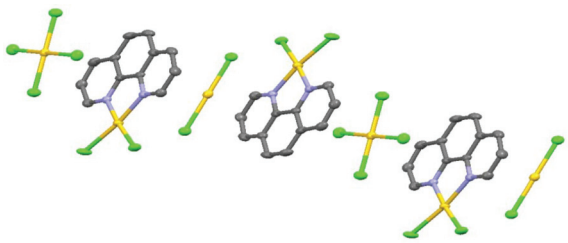

Fig. 5 An ellipsoid plot visualized with Mercury[56] to show extended linearized placement of gold atoms. Each counterion sits on a crystallographic inversion center. All non-hydrogen atoms are drawn at 50% probability. H atoms are omitted to enhance clarity.

refined by full-matrix least-squares to give R_1 = 0.0193. This novel compound also crystallizes in the space group $P\bar{1}$, with an asymmetric unit containing one coordinated phenanthroline Au(III) complex cation and two half $[AuCl_2]^{-1}$ anions. The Au1–N1 (2.037(4) Å) and Au1–N2 (2.041(4) Å) bond lengths are also comparable to the Au–N bond lengths found in other four-coordinate Au(III) amine complexes, such as $[Au(dien)Cl]_2$ and $[Au(en)(SO_3)_2]$, which exhibit typical bond lengths between 1.97 and 2.14 Å.[53,54] The typical Au–Cl bond distance (2.26–2.42 Å)[53,55] can also be observed for the structure with each respective Au–Cl bond distance being 2.2571(1) Å and 2.2595(12) Å.

The novel mixed valence Au(III) crystal (0.070 × 0.060 × 0.030 mm) structure (**2**) was solved using Mo Kα radiation at 90.0(2)K. Structure refinement by full-matrix least-squares analysis converged to an R_1 value of 0.0150. This molecule is shown to crystallize in the triclinic crystal system, space group $P\bar{1}$. The asymmetric unit of the mixed valence compound contains one $[Au(phen)Cl_2]^+$ cation, half of one $[AuCl_4]^{-1}$ counterion and half of a linear $[AuCl_2]^{-1}$ counterion. Each anion lies on an inversion center, which leads to the formula $[Au(phen)Cl_2]_2[AuCl_4][AuCl_2]$ (Fig. 5).

Conclusion

In summary, we used a rapid temperature-controlled method to synthesize new *N*,*N*-bipyridyl ligated Au(III) centers with mixed valence character. The approach circumvents protonated bipyridyl salts that compete with the desired product following literature protocols that use high temperature for 4 h. X-ray crystallography sheds light on the structural character of these complexes, particularly on those with gold counteranions. Complexes **1** and **2** crystallize in a unit cell with low symmetry in comparison with **5** and **6**, which crystallize in a monoclinic crystal system. Complex **3** exhibits a much higher order of symmetry, space group *Pbca*, and is consistent with **7**, which has been reported by Ferraz de Paiva *et al.*[48] Additionally, variable temperature NMR studies support the rationale for the studies as high temperatures shift the equilibrium to the formation of protonated bipyridyl salts over the desired coordinated products and that the process is irreversible. This report offers a facile and relatively fast method to access mononuclear Au(III) complexes bearing *N*,*N*-bidentate ligands and reactivity of $HAuCl_4$ in solution without protonolysis.

Conflicts of interest

The authors state that there are no conflicts to declare.

Acknowledgements

Financial support was provided by the University of Kentucky (UK). This study made use of the UK NMR facility, the UK X-ray facility with funds from the MRI program (grants CHE-0319176 and CHE-1625732), and Boston University Mass spectrometry facility. We thank Dr. Justin Mobley for assistance with VT-NMR.

Notes and references

1 P. Schwerdtfeger, *Heteroat. Chem.*, 2002, **13**, 578–584.
2 R. Coquet, K. L. Howard and D. J. Willock, *Chem. Soc. Rev.*, 2008, **37**, 2046–2076.
3 P. Pyykko, *Chem. Rev.*, 1988, **88**, 563–594.
4 D. J. Gorin and F. D. Toste, *Nature*, 2007, **446**, 395.
5 R. Dorel and A. M. Echavarren, *Chem. Rev.*, 2015, **115**, 9028–9072.
6 Y. Shi, K. E. Roth, S. D. Ramgren and S. A. Blum, *J. Am. Chem. Soc.*, 2009, **131**, 18022–18023.
7 L. Rocchigiani, J. Fernandez-Cestau, G. Agonigi, I. Chambrier, P. H. M. Budzelaar and M. Bochmann, *Angew. Chem., Int. Ed.*, 2017, **56**, 13861–13865.
8 R. Kumar and C. Nevado, *Angew. Chem., Int. Ed.*, 2017, **56**, 1994–2015.
9 M. W. Johnson, A. G. DiPasquale, R. G. Bergman and F. D. Toste, *Organometallics*, 2014, **33**, 4169–4172.
10 S. Carotti, A. Guerri, T. Mazzei, L. Messori, E. Mini and P. Orioli, *Inorg. Chim. Acta*, 1998, **281**, 90–94.
11 S. Zhu, W. Gorski, D. R. Powell and J. A. Walmsley, *Inorg. Chem.*, 2006, **45**, 2688–2694.
12 V. Amani, A. Abedi, S. Ghabeshi, H. R. Khavasi, S. M. Hosseini and N. Safari, *Polyhedron*, 2014, **79**, 104–115.
13 A. Casini, M. C. Diawara, R. Scopelliti, S. M. Zakeeruddin, M. Grätzel and P. J. Dyson, *Dalton Trans.*, 2010, **39**, 2239–2245.

14 C. Topf, C. Hirtenlehner, M. Zabel, M. List, M. Fleck and U. Monkowius, *Organometallics*, 2011, **30**, 2755–2764.
15 G. Marcon, S. Carotti, M. Coronnello, L. Messori, E. Mini, P. Orioli, T. Mazzei, M. A. Cinellu and G. Minghetti, *J. Med. Chem.*, 2002, **45**, 1672–1677.
16 M. Altaf, M. Monim-Ul-Mehboob, A.-N. Kawde, G. Corona, R. Larcher, M. Ogasawara, N. Casagrande, M. Celegato, C. Borghese, Z. H. Siddik, D. Aldinucci and A. A. Isab, *Oncotarget*, 2016, **8**, 490–505.
17 R. Cai, M. Lu, E. Y. Aguilera, Y. Xi, N. G. Akhmedov, J. L. Petersen, H. Chen and X. Shi, *Angew. Chem., Int. Ed. Engl.*, 2015, **54**, 8772–8776.
18 M. J. Harper, C. J. Arthur, J. Crosby, E. J. Emmett, R. L. Falconer, A. J. Fensham-Smith, P. J. Gates, T. Leman, J. E. McGrady, J. F. Bower and C. A. Russell, *J. Am. Chem. Soc.*, 2018, **140**, 4440–4445.
19 A. Casini, M. A. Cinellu, G. Minghetti, C. Gabbiani, M. Coronnello, E. Mini and L. Messori, *J. Med. Chem.*, 2006, **49**, 5524–5531.
20 M. A. Cinellu, L. Maiore, M. Manassero, A. Casini, M. Arca, H.-H. Fiebig, G. Kelter, E. Michelucci, G. Pieraccini, C. Gabbiani and L. Messori, *ACS Med. Chem. Lett.*, 2010, **1**, 336–339.
21 B. P. Block and J. C. Bailar, *J. Am. Chem. Soc.*, 1951, **73**, 4722–4725.
22 R. Ahmadi, V. Amani and H. R. Khavasi, *Acta Crystallogr., Sect. E: Struct. Rep. Online*, 2008, **64**, m1156–m1157.
23 S. Karaca, M. Akkurt, N. Safari, V. Amani, O. Buyukgungor and A. Abedi, *Acta Crystallogr., Sect. E: Struct. Rep. Online*, 2009, **65**, m335–m336.
24 L. S. Hollis and S. J. Lippard, *J. Am. Chem. Soc.*, 1983, **105**, 4293–4299.
25 L. Pazderski, J. Toušek, J. Sitkowski, L. Kozerski, R. Marek and E. Szłyk, *Magn. Reson. Chem.*, 2007, **45**, 24–36.
26 X.-P. Zhang, G. Yang, L. Wang and S. W. Ng, *Acta Crystallogr., Sect. E: Struct. Rep. Online*, 2007, **63**, m1582.
27 S. O. Yildirim, M. Akkurt, N. Safari, V. Amani, V. McKee, A. Abedi and H. R. Khavasi, *Acta Crystallogr., Sect. E: Struct. Rep. Online*, 2008, **64**, m1189–m1190.
28 E. J. L. McInnes, A. J. Welch and L. J. Yellowlees, *Acta Crystallogr., Sect. C: Cryst. Struct. Commun.*, 1995, **51**, 2023–2025.
29 G. Annibale, L. Canovese, L. Cattalini, G. Natile, M. Biagini-Cingi, A.-M. Manotti-Lanfredi and A. Tiripicchio, *J. Chem. Soc., Dalton Trans.*, 1981, 2280–2287.
30 A. J. Canty, N. J. Minchin, P. C. Healy and A. H. White, *J. Chem. Soc., Dalton Trans.*, 1982, 1795–1802.
31 C. M. Harris, *J. Chem. Soc.*, 1959, 682–687.
32 G. D. Dimitrov and M. V. Neykov, *Spectrochim. Acta, Part A*, 2007, **68**, 399–403.
33 B. Milani, A. Anzilutti, L. Vicentini, A. Sessanta o Santi, E. Zangrando, S. Geremia and G. Mestroni, *Organometallics*, 1997, **16**, 5064–5075.
34 S. Parkin and H. Hope, *J. Appl. Crystallogr.*, 1998, **31**, 945–953.
35 H. Hope, *Prog. Inorg. Chem.*, 1994, **41**, 1–19.
36 Bruker, *APEX2*, Bruker-AXS, Madison, WI, USA, 2006.
37 L. Krause, R. Herbst-Irmer, G. M. Sheldrick and D. Stalke, *J. Appl. Crystallogr.*, 2015, **48**, 3–10.
38 G. M. Sheldrick, *SADABS, Program for bruker area detector absorption correction*, University of Gottingen, Gottingen, 1997.
39 G. M. Sheldrick, *Acta Crystallogr., Sect. C: Struct. Chem.*, 2015, **71**, 3–8.
40 G. M. Sheldrick, *Acta Crystallogr., Sect. A: Found. Adv.*, 2015, **71**, 3–8.
41 G. Sheldrick, *Acta Crystallogr., Sect. A: Found. Crystallogr.*, 2008, **64**, 112–122.
42 A. L. Spek, *Acta Crystallogr., Sect. D: Biol. Crystallogr.*, 2009, **65**, 148–155.
43 S. Parkin, *Acta Crystallogr., Sect. A: Found. Crystallogr.*, 2000, **56**, 317.
44 N. S. Radulović, N. M. Stojanović, B. Đ. Glišić, P. J. Randjelović, Z. Z. Stojanović-Radić, K. V. Mitić, M. G. Nikolić and M. I. Djuran, *Polyhedron*, 2018, **141**, 164–180.
45 D. M. Motley, J. A. Walmsley, J. Zukerman-Schpector and E. R. T. Tiekink, *J. Chem. Crystallogr.*, 2009, **39**, 364–367.
46 Z. D. Hudson, C. D. Sanghvi, M. A. Rhine, J. J. Ng, S. D. Bunge, K. I. Hardcastle, M. R. Saadein, C. E. MacBeth and J. F. Eichler, *Dalton Trans.*, 2009, 7473–7480.
47 F. Abbate, P. Orioli, B. Bruni, G. Marcon and L. Messori, *Inorg. Chim. Acta*, 2000, **311**, 1–5.
48 R. E. Ferraz de Paiva, D. H. Nakahata and P. P. Corbi, *Acta Crystallogr., Sect. E: Crystallogr. Commun.*, 2017, **73**, 1048–1051.
49 W. H. Baddley, F. Basolo, H. B. Gray, C. Nolting and A. J. Poe, *Inorg. Chem.*, 1963, **2**, 921–928.
50 H.-N. Adams and J. Strähle, *Z. Anorg. Allg. Chem.*, 1982, **485**, 65–80.
51 D. Paliwoda, M. Szafrański, M. Hanfland and A. Katrusiak, *J. Mater. Chem. C*, 2018, **6**, 7689–7699.
52 J. A. Krause, D. Zhao, S. Chatterjee, R. Falcon, K. Stoltz, J. C. Warren, S. E. Wiswell, W. B. Connick and S. N. Collins, *Acta Crystallogr., Sect. C: Struct. Chem.*, 2014, **70**, 260–266.
53 G. Nardin, L. Randaccio, G. Annibale, G. Natile and B. Pitteri, *J. Chem. Soc., Dalton Trans.*, 1980, 220–223.
54 A. Dunand and R. Gerdil, *Acta Crystallogr., Sect. B: Struct. Crystallogr. Cryst. Chem.*, 1975, **31**, 370–374.
55 W. T. Robinson and E. Sinn, *J. Chem. Soc., Dalton Trans.*, 1975, 726–731.
56 C. F. Macrae, I. J. Bruno, J. A. Chisholm, P. R. Edgington, P. McCabe, E. Pidcock, L. Rodriguez-Monge, R. Taylor, J. Van De Streek and P. A. Wood, *J. Appl. Crystallogr.*, 2008, **41**, 466–470.